

# Combined analysis of the $\pi^- p \rightarrow K^0 \Lambda$ , $\eta n$ reactions in a chiral quark model

Li-Ye Xiao, Fan Ouyang and Xian-Hui Zhong \*

1) Department of Physics, Hunan Normal University, Changsha 410081, China

2) Synergetic Innovation Center for Quantum Effects and Applications (SICQEA), Changsha 410081, China and

3) Key Laboratory of Low-Dimensional Quantum Structures and Quantum Control of Ministry of Education, Changsha 410081, China

A combined analysis of the reactions  $\pi^- p \rightarrow K^0 \Lambda$  and  $\eta n$  is carried out with a chiral quark model. The data in the center-of-mass (c.m.) energy range from threshold up to  $W \simeq 1.8$  GeV are reasonably described. For  $\pi^- p \rightarrow K^0 \Lambda$ , it is found that  $N(1535)S_{11}$  and  $N(1650)S_{11}$  play crucial roles near threshold. The  $N(1650)S_{11}$  resonance contributes to the reaction through configuration mixing with  $N(1535)S_{11}$ . The constructive interference between  $N(1535)S_{11}$  and  $N(1650)S_{11}$  is responsible for the peak structure around threshold in the total cross section. The  $n$ -pole,  $u$ - and  $t$ -channel backgrounds provide significant contributions to the reaction as well. While, for the  $\pi^- p \rightarrow \eta n$  process, the “first peak” in the total cross section is dominant by  $N(1535)S_{11}$ , which has a sizeable destructive interference with  $N(1650)S_{11}$ . Around  $P_\pi \simeq 1.0$  GeV/c ( $W \simeq 1.7$  GeV), there seems to be a small bump structure in the total cross section, which might be explained by the interference between the  $u$ -channel and  $N(1650)S_{11}$ . The  $N(1520)D_{13}$  resonance notably affects the angle distributions of the cross sections, although less effects are seen in the total cross section. The role of  $P$ -wave state  $N(1720)P_{13}$  should be further confirmed by future experiments. If  $N(1720)P_{13}$  has a narrow width of  $\Gamma \simeq 120$  MeV as found in our previous work by a study of the  $\pi^0$  photoproduction processes, obvious evidence should be seen in the  $\pi^- p \rightarrow K^0 \Lambda$  and  $\eta n$  processes as well.

PACS numbers: 13.75.Gx; 14.20.Gk.; 12.39.Jh

## I. INTRODUCTION

Understanding of the baryon spectrum and searching for the missing nucleon resonances and new exotic states are favored topics in hadronic physics [1]. Pion-nucleon ( $\pi N$ ) scattering provides us an important tool to study the light baryon spectrum. Most of our current knowledge about the nucleon resonances listed in the Review of Particle Physics by the Particle Data Group (PDG) [2] was extracted from partial wave analyses of the  $\pi N$  scattering. As we know, in the constituent quark model a rich spectrum of nucleon resonances is predicted [3–5], however, some of them are still missing. To look for the missing resonances and deal with the unresolved issues in hadronic physics, more precise measurements of pion-induced reactions are suggested recently in Ref. [6], meanwhile, reliable partial wave analyses are the same important as the precise measurements for us to extract the information on resonance properties.

In the  $\pi N$  scattering, the  $\pi^- p \rightarrow K^0 \Lambda$  and  $\eta n$  reactions are of special interest in hadronic physics. The reasons are as follows. i) Only the baryon resonances with isospin  $I = 1/2$  contribute to these two reactions due to the isospin selection rule. Thus, the  $\pi^- p \rightarrow K^0 \Lambda$  and  $\eta n$  processes provide us a rather clear place to extract the properties of nucleon resonances without interferences from the  $\Delta^*$  states. ii) The  $\pi^- p \rightarrow K^0 \Lambda$  and  $\eta n$  reactions can let us obtain information on strong couplings of nucleon resonances to  $K\Lambda$  and  $\eta N$  channels, which can not be obtained in the elastic  $\pi N$  scattering. iii) Furthermore, in these reactions one may find evidence of some resonances which couple only weakly to the  $\pi N$  channel. Hence, many studies about these two reactions have been carried out.

In experiments, some measurements of  $\pi^- p \rightarrow K^0 \Lambda$  and  $\eta n$  were carried out about 20 or 30 years ago, the data had been collected in [7]. For the  $\pi^- p \rightarrow K^0 \Lambda$  reaction, the data of total cross section and differential cross sections can be obtained in the whole resonance range [8–15], furthermore, some data of  $\Lambda$  polarization are also obtained in the energy region  $W < 1.8$  GeV [11]. While for the  $\pi^- p \rightarrow \eta n$  reaction, a few precise data on the differential cross sections and total cross section can be obtained near the  $N(1535)S_{11}$  mass threshold from Crystal Ball spectrometer at BNL [16], however, other old data [17–22] might be problematic over the whole energy range for its limited angle coverage and uncontrollable uncertainties [23]. Thus, to get reliable information on the resonance properties, a combined analysis of the  $\pi^- p \rightarrow K^0 \Lambda$  and  $\eta n$  reactions is necessary before new precise data are obtained.

In theory, various theoretical approaches have been applied to analyze the  $\pi^- p \rightarrow K^0 \Lambda$  and/or  $\eta n$  reactions, such as the chiral unitary model [24],  $K$ -matrix methods [25–35], dynamical coupled-channel models [7, 36–41], the BnGa approach [42], chiral quark model [43, 44], and other effective approaches [45–47], etc. However, the analyses from different models claim a different resonance content in the reactions [6]. For example, in  $\pi^- p \rightarrow K^0 \Lambda$  reaction the large peak near  $W = 1.7$  GeV is explained as the dominant contributions from both  $N(1650)S_{11}$  and  $N(1710)P_{11}$  in Ref. [25]; from  $N(1720)P_{13}$  in Ref. [27]; however, from  $N(1535)S_{11}$ ,  $N(1650)S_{11}$  and  $N(1720)P_{13}$  in Ref. [45]. While in  $\pi^- p \rightarrow \eta n$  reaction, the second bump structure near  $W = 1.7$  GeV is explained as the dominant contributions of  $N(1710)P_{11}$  in Refs. [7, 27, 29]; in Ref. [44] it is argued that this structure is mainly caused by  $N(1720)P_{13}$ ; however, in Ref. [40, 41] it is predicted that this structure is due to the interference between  $N(1535)S_{11}$  and  $N(1650)S_{11}$ . To clarify these puzzles in the reactions, more theoretical studies are needed.

In this work, we carry a combined study of  $\pi^- p \rightarrow K^0 \Lambda$

\*E-mail: zhongxh@hunnu.edu.cn

and  $\eta n$  reactions within a chiral quark model. Firstly, we hope to obtain a better understanding of the reaction mechanism for these reactions. In our previous work [43], we first extended the chiral quark model to study of the  $\pi^- p \rightarrow \eta n$  reaction, where we only obtained reasonable results near threshold. In order to further understand the reaction at higher resonance region and get more solid predictions, we need revisit this reaction by combining with the reaction  $\pi^- p \rightarrow K^0 \Lambda$ . Secondly, we expect to further confirm the extracted properties of  $N(1535)S_{11}$  from the  $\eta$ - and  $\pi$ -meson photoproduction processes in our previous works [48, 49]. Where we predicted that  $N(1535)S_{11}$  might be explained as a mixing three-quark state between representations of  $[70,^2 8]$  and  $[70,^4 8]$  in the quark model. However, in the literature it is argued that it may contain a large admixture of pentaquark component for its large couplings to  $\eta N$  and  $K\Lambda$  channels [50, 51]. The  $N(1535)S_{11}$  resonance is also considered as a dynamically generated state in the chiral unitary models [52–55]. Finally, we hope to extract some information on  $N(1720)P_{13}$  in the  $\pi^- p \rightarrow K^0 \Lambda$  and  $\eta n$  reactions and test its properties obtained by us in the  $\pi$ -meson photoproduction processes, where we found the  $N(1720)P_{13}$  resonance might favor a narrow width of  $\Gamma \simeq 120$  MeV [49], which about a factor of 2 narrower than the world average value from PDG [2].

In the chiral quark model, an effective chiral Lagrangian is introduced to account for the quark-pseudoscalar-meson coupling. Since the quark-meson coupling is invariant under the chiral transformation, some of the low-energy properties of QCD are retained. There are several outstanding features for this model [43]. One is that only a very limited number of adjustable parameters will appear in this framework. In particular, only one overall parameter is needed for the nucleon resonances to be coupled to the pseudoscalar mesons in the  $SU(6) \otimes O(3)$  symmetry limit. This distinguishes from hadronic models where each resonance requires one additional coupling constant as free parameter. Another one is that all the nucleon resonances can be treated consistently in the quark model. Thus, it has predictive powers when exposed to experimental data, and information about the resonance structures can be extracted. The chiral quark model has been well developed and widely applied to meson photoproduction reactions [48, 49, 56–68]. Recently, this model has been successfully extended to  $\pi N$  and  $KN$  reactions as well [43, 69–71].

This work is organized as follows. The model is reviewed in Sec.II. Then, in Sec.III, our numerical results and analyses are presented and discussed. Finally, a summary is given in Sec.IV.

## II. FRAMEWORK

In this section, we give a brief review of the chiral quark model. In this model, the  $s$ - and  $u$ -channel transition amplitudes can be expressed as [43]

$$\mathcal{M}_s = \sum_j \langle N_f | H_m^f | N_j \rangle \langle N_j | \frac{1}{E_i + \omega_i - E_j} H_m^i | N_i \rangle, \quad (1)$$

TABLE I:  $g$  factors extracted in the symmetric quark model.

Factor	$\pi^- p \rightarrow K^0 \Lambda$	$\pi^- p \rightarrow \eta n$
$g_{s1}$	$\frac{\sqrt{6}}{2}$	1.0
$g_{s2}$	$\frac{\sqrt{6}}{3}$	$\frac{2}{3}$
$g_{v1}$	$\frac{\sqrt{6}}{2}$	$\frac{5}{3}$
$g_{v2}$	$\frac{\sqrt{6}}{3}$	0.0
$g_{s1}^\mu$	0.0	1.0
$g_{s2}^\mu$	$\frac{\sqrt{6}}{3}$	$\frac{2}{3}$
$g_{v1}^\mu$	0.0	$\frac{5}{3}$
$g_{v2}^\mu$	$-\frac{\sqrt{6}}{3}$	0.0
$g_t^s$	$\frac{\sqrt{6}}{2}$	1.0
$g_t^v$	$\frac{\sqrt{6}}{2}$	$\frac{5}{3}$

$$\mathcal{M}_u = \sum_j \langle N_f | H_m^i \frac{1}{E_i - \omega_i - E_j} | N_j \rangle \langle N_j | H_m^f | N_i \rangle, \quad (2)$$

where  $H_m^i$  and  $H_m^f$  stand for the incoming and outgoing meson-quark couplings, respectively. They might be described by the effective chiral Lagrangian [59, 60],

$$H_m = \frac{1}{f_m} \bar{\psi}_j \gamma_\mu^j \gamma_5^j \psi_j \vec{\tau} \cdot \partial^\mu \vec{\phi}_m, \quad (3)$$

where  $\psi_j$  represents the  $j$ -th quark field in a hadron,  $f_m$  is the meson's decay constant, and  $\phi_m$  is the field of the pseudoscalar-meson octet. The  $\omega_i$  and  $\omega_f$  are the energies of the incoming and outgoing mesons, respectively.  $|N_i\rangle$ ,  $|N_j\rangle$  and  $|N_f\rangle$  stand for the initial, intermediate, and final states, respectively, and their corresponding energies are  $E_i$ ,  $E_j$ , and  $E_f$ , which are the eigenvalues of the nonrelativistic Hamiltonian of the constituent quark model  $\hat{H}$  [3, 4]. The  $s$ - and  $u$ -channel transition amplitudes have been worked out in the harmonic oscillator basis in Refs. [43, 70, 71], and the  $g$  factors appearing in the  $s$ - and  $u$ -channel amplitudes have been defined in Ref. [70], whose values are worked out and listed in Table I.

The  $t$ -channel contributions of vector and/or scalar exchanges are included in this work. The vector meson-quark and scalar meson-quark couplings are give by

$$H_V = \bar{\psi}_j \left( a \gamma^\nu + \frac{b \sigma^{\nu\lambda} \partial_\lambda}{2m_q} \right) V_\nu \psi_j, \quad (4)$$

$$H_S = g_{Sqq} \bar{\psi}_j \psi_j S, \quad (5)$$

where  $V$  and  $S$  stand for the vector and scalar fields, respectively. The constants  $a$ ,  $b$ , and  $g_{Sqq}$  are vector, tensor, and scalar coupling constants, respectively. They are treated as free parameters in this work.

Meanwhile, the  $VPP$  and  $SPP$  couplings ( $P$  stands for a pseudoscalar-meson) are adopted as

$$H_{VPP} = -iG_V Tr([\phi_m, \partial_\mu \phi_m] V^\mu), \quad (6)$$

$$H_{SPP} = \frac{g_{SPP}}{2m_\pi} \partial_\mu \phi_m \partial^\mu \phi_m S, \quad (7)$$

TABLE II: The  $s$ -channel resonance amplitudes within  $n=2$  shell for the  $\pi^- p \rightarrow K^0 \Lambda, \eta n$  processes. We have defined  $M_S \equiv \left[ \frac{\omega_i}{\mu_q} - |\mathbf{A}_{\text{in}}| \frac{2|\mathbf{k}|}{3\alpha^2} \right] \left[ \frac{\omega_f}{\mu_q} - |\mathbf{A}_{\text{out}}| \frac{2|\mathbf{q}|}{3\alpha^2} \right]$ ,  $M_P = M_D \equiv \frac{|\mathbf{A}_{\text{out}}||\mathbf{A}_{\text{in}}|}{|\mathbf{k}||\mathbf{q}|}$ ,  $M_{P0} \equiv \left[ \frac{\omega_i}{\mu_q} - |\mathbf{A}_{\text{in}}| \frac{|\mathbf{k}|}{\alpha^2} \right] \left[ \frac{\omega_f}{\mu_q} - |\mathbf{A}_{\text{out}}| \frac{|\mathbf{q}|}{\alpha^2} \right]$ ,  $M_{P2} \equiv \left[ \frac{\omega_i}{\mu_q} - |\mathbf{A}_{\text{in}}| \frac{2|\mathbf{k}|}{3\alpha^2} \right] \left[ \frac{\omega_f}{\mu_q} - |\mathbf{A}_{\text{out}}| \frac{2|\mathbf{q}|}{3\alpha^2} \right]$ ,  $M_F \equiv \frac{|\mathbf{A}_{\text{out}}||\mathbf{A}_{\text{in}}|}{\alpha^4}$ ,  $P'_l(z) \equiv \frac{\partial P_l(z)}{\partial z}$ ,  $X_{S1} \equiv [\cos \theta_S + \sin \theta_S] [2 \cos \theta_S - \sin \theta_S]$ ,  $X_{S2} \equiv [\sin \theta_S - \cos \theta_S] [2 \sin \theta_S + \cos \theta_S]$ . The functions  $\mathbf{A}_{\text{in}}$  and  $\mathbf{A}_{\text{out}}$  have been defined in [71]. The  $\mu_q$  is a reduced mass at the quark level, which equals to  $1/\mu_q = 1/m_u + 1/m_s$  for  $K$  productions, while  $1/\mu_q = 2/m_u$  for  $\eta$  productions.  $P_l(z)$  is the Legendre function with  $z = \cos \theta$ .

$[N_6, {}^{2S+1}N_3, n, I]$	$l_{2I, 2J}$	$O_R$	$\pi^- p \rightarrow K^0 \Lambda$	$\pi^- p \rightarrow \eta n$
$[70, {}^2 8, 0, 0]$	$P_{11}(n)$	$f(\theta)$ $g(\theta)$	$\frac{5}{\sqrt{6}} M_P  \mathbf{k}  \mathbf{q}  P_1(z)$ $\frac{5}{\sqrt{6}} M_P  \mathbf{k}  \mathbf{q}  \sin \theta P'_1(z)$	$\frac{5}{3} M_P  \mathbf{k}  \mathbf{q}  P_1(z)$ $\frac{5}{3} M_P  \mathbf{k}  \mathbf{q}  \sin \theta P'_1(z)$
$+ \cos \theta_S [70, {}^2 8, 1, 1]$	$N(1535)S_{11}$	$f(\theta)$	$\frac{\sqrt{6}}{12} \cos^2 \theta_S M_S \alpha^2$	$\frac{1}{6} X_{S1} M_S \alpha^2$
$- \sin \theta_S [70, {}^4 8, 1, 1]$		$g(\theta)$	—	—
$+ \cos \theta_S [70, {}^4 8, 1, 1]$	$N(1650)S_{11}$	$f(\theta)$	$\frac{\sqrt{6}}{12} \sin^2 \theta_S M_S \alpha^2$	$\frac{1}{6} X_{S2} M_S \alpha^2$
$+ \sin \theta_S [70, {}^2 8, 1, 1]$		$g(\theta)$	—	—
$[70, {}^2 8, 1, 1]$	$N(1520)D_{13}$	$f(\theta)$ $g(\theta)$	$\frac{20\sqrt{6}}{27} M_D \frac{ \mathbf{k}  \mathbf{q} }{\alpha^2} P_2(z)$ $\frac{10\sqrt{6}}{27} M_D \frac{ \mathbf{k}  \mathbf{q} }{\alpha^2} \sin(\theta) P'_2(z)$	$\frac{76}{135} M_D \frac{ \mathbf{k}  \mathbf{q} }{\alpha^2} P_2(z)$ $\frac{38}{135} M_D \frac{ \mathbf{k}  \mathbf{q} }{\alpha^2} \sin \theta P'_2(z)$
$[70, {}^4 8, 1, 1]$	$N(1700)D_{13}$	$f(\theta)$ $g(\theta)$	— —	$-\frac{38}{1350} M_D \frac{ \mathbf{k}  \mathbf{q} }{\alpha^2} P_2(z)$ $-\frac{19}{1350} M_D \frac{ \mathbf{k}  \mathbf{q} }{\alpha^2} \sin \theta P'_2(z)$
	$N(1675)D_{15}$	$f(\theta)$ $g(\theta)$	— —	$-\frac{2}{15} M_D \frac{ \mathbf{k}  \mathbf{q} }{\alpha^2} P_2(z)$ $\frac{2}{45} M_D \frac{ \mathbf{k}  \mathbf{q} }{\alpha^2} \sin \theta P'_2(z)$
$[56, {}^2 8, 2, 0]$	$N(1440)P_{11}$	$f(\theta)$ $g(\theta)$	$\frac{5\sqrt{6}}{24 \times 27} M_{P0}  \mathbf{k}  \mathbf{q}  P_1(z)$ $\frac{5\sqrt{6}}{24 \times 27} M_{P0}  \mathbf{k}  \mathbf{q}  \sin \theta P'_1(z)$	$\frac{5}{12 \times 27} M_{P0}  \mathbf{k}  \mathbf{q}  P_1(z)$ $\frac{5}{12 \times 27} M_{P0}  \mathbf{k}  \mathbf{q}  \sin \theta P'_1(z)$
$[70, {}^2 8, 2, 0]$	$N(1710)P_{11}$	$f(\theta)$ $g(\theta)$	$\frac{2\sqrt{6}}{24 \times 27} M_{P0}  \mathbf{k}  \mathbf{q}  P_1(z)$ $\frac{2\sqrt{6}}{24 \times 27} M_{P0}  \mathbf{k}  \mathbf{q}  \sin \theta P'_1(z)$	$\frac{1}{3 \times 27} M_{P0}  \mathbf{k}  \mathbf{q}  P_1(z)$ $\frac{1}{3 \times 27} M_{P0}  \mathbf{k}  \mathbf{q}  \sin \theta P'_1(z)$
$[70, {}^4 8, 2, 2]$	$N(1880)P_{11}$	$f(\theta)$ $g(\theta)$	— —	$-\frac{5}{4 \times 81} M_{P2}  \mathbf{k}  \mathbf{q}  P_1(z)$ $-\frac{5}{4 \times 81} M_{P2}  \mathbf{k}  \mathbf{q}  \sin \theta P'_1(z)$
$[70, {}^4 8, 2, 0]$	$N(?)P_{13}$	$f(\theta)$ $g(\theta)$	— —	$-\frac{1}{2 \times 81} M_{P0}  \mathbf{k}  \mathbf{q}  P_1(z)$ $\frac{1}{4 \times 81} M_{P0}  \mathbf{k}  \mathbf{q}  \sin \theta P'_1(z)$
$[56, {}^2 8, 2, 2]$	$N(1720)P_{13}$	$f(\theta)$ $g(\theta)$	$\frac{25\sqrt{6}}{24 \times 27} M_{P2}  \mathbf{k}  \mathbf{q}  P_1(z)$ $-\frac{25\sqrt{6}}{48 \times 27} M_{P2}  \mathbf{k}  \mathbf{q}  \sin \theta P'_1(z)$	$\frac{25}{4 \times 81} M_{P2}  \mathbf{k}  \mathbf{q}  P_1(z)$ $-\frac{25}{8 \times 81} M_{P2}  \mathbf{k}  \mathbf{q}  \sin \theta P'_1(z)$
$[70, {}^2 8, 2, 2]$	$N(1900)P_{13}$	$f(\theta)$ $g(\theta)$	$\frac{10\sqrt{6}}{24 \times 27} M_{P2}  \mathbf{k}  \mathbf{q}  P_1(z)$ $-\frac{10\sqrt{6}}{48 \times 27} M_{P2}  \mathbf{k}  \mathbf{q}  \sin \theta P'_1(z)$	$\frac{5}{81} M_{P2}  \mathbf{k}  \mathbf{q}  P_1(z)$ $-\frac{5}{2 \times 81} M_{P2}  \mathbf{k}  \mathbf{q}  \sin \theta P'_1(z)$
$[70, {}^4 8, 2, 2]$	$N(?)P_{13}$	$f(\theta)$ $g(\theta)$	— —	$-\frac{5}{4 \times 81} M_{P2}  \mathbf{k}  \mathbf{q}  P_1(z)$ $\frac{5}{8 \times 81} M_{P2}  \mathbf{k}  \mathbf{q}  \sin \theta P'_1(z)$
$[56, {}^2 8, 2, 2]$	$N(1680)F_{15}$	$f(\theta)$ $g(\theta)$	$\frac{3\sqrt{6}}{4} M_F  \mathbf{k}  \mathbf{q}  P_3(z)$ $\frac{\sqrt{6}}{4} M_F  \mathbf{k}  \mathbf{q}  P'_3(z)$	$\frac{3}{2} M_F  \mathbf{k}  \mathbf{q}  P_3(z)$ $\frac{1}{2} M_F  \mathbf{k}  \mathbf{q}  \sin \theta P'_3(z)$
$[70, {}^2 8, 2, 2]$	$N(1860)F_{15}$	$f(\theta)$ $g(\theta)$	$\frac{3\sqrt{6}}{10} M_F  \mathbf{k}  \mathbf{q}  P_3(z)$ $\frac{\sqrt{6}}{10} M_F  \mathbf{k}  \mathbf{q}  \sin \theta P'_3(z)$	$\frac{6}{5} M_F  \mathbf{k}  \mathbf{q}  P_3(z)$ $\frac{2}{5} M_F  \mathbf{k}  \mathbf{q}  \sin \theta P'_3(z)$
$[70, {}^4 8, 2, 2]$	$N(?)F_{15}$	$f(\theta)$ $g(\theta)$	— —	$-\frac{3}{35} M_F  \mathbf{k}  \mathbf{q}  P_3(z)$ $-\frac{1}{35} M_F  \mathbf{k}  \mathbf{q}  \sin \theta P'_3(z)$
$[70, {}^4 8, 2, 2]$	$N(?)F_{17}$	$f(\theta)$ $g(\theta)$	— —	$-\frac{18}{35} M_F  \mathbf{k}  \mathbf{q}  P_4(z)$ $\frac{9}{70} M_F  \mathbf{k}  \mathbf{q}  \sin \theta P'_3(z)$

where  $G_V$  and  $g_{SPP}$  are the  $VPP$  and  $SPP$  coupling constants, respectively, to be determined by experimental data.

The  $t$ -channel transition amplitude has been given in Ref. [71]. In this work, the scalar  $\kappa$ -meson and vector  $K^*$ -meson exchanges are considered for the  $\pi^- p \rightarrow K^0 \Lambda$  process, while the scalar  $a_0(980)$ -meson exchange is considered for the  $\pi^- p \rightarrow \eta n$  process.

It should be pointed out that the amplitudes in terms of the harmonic oscillator principle quantum number  $n$  are sum of a set of SU(6) multiplets with the same  $n$ . To obtain the contri-

butions of individual resonances, we need to separate out the single-resonances-excitation amplitudes within each principle number  $n$  in the  $s$  channel. Taking into account the width effects of the resonances, the resonance transition amplitudes of  $s$  channel can be generally expressed as [43, 71]

$$\mathcal{M}_R^s = \frac{2M_R}{s - M_R^2 + iM_R\Gamma_R} O_R e^{-(\mathbf{k}^2 + \mathbf{q}^2)/6\alpha^2}, \quad (8)$$

where  $\sqrt{s} = E_i + \omega_i$  is the total energy of the system;  $\mathbf{k}$  and  $\mathbf{q}$  stand for the momenta of incoming and outgoing mesons,

respectively;  $\alpha$  is the harmonic oscillator strength;  $O_R$  is the separated operators for individual resonances in the  $s$  channel; and  $M_R$  is the mass of the  $s$ -channel resonance with a width  $\Gamma_R$ . The transition amplitudes can be written in a standard form [72]:

$$O_R = f(\theta) + ig(\theta)\boldsymbol{\sigma} \cdot \mathbf{n}, \quad (9)$$

where  $\boldsymbol{\sigma}$  is the spin operator of the nucleon, while  $\mathbf{n} \equiv \mathbf{q} \times \mathbf{k}/|\mathbf{k} \times \mathbf{q}|$ .  $f(\theta)$  and  $g(\theta)$  stand for the non-spin-flip and spin-flip amplitudes, respectively, which can be expanded in terms of the familiar partial wave amplitudes  $T_{l\pm}$  for the states with  $J = l \pm 1/2$ :

$$f(\theta) = \sum_{l=0}^{\infty} [(l+1)T_{l+} + lT_{l-}] P_l(\cos \theta), \quad (10)$$

$$g(\theta) = \sum_{l=0}^{\infty} [T_{l-} - T_{l+}] \sin \theta P'_l(\cos \theta), \quad (11)$$

where  $\theta$  is the scattering angle between  $\mathbf{k}$  and  $\mathbf{q}$ .

We have extracted the scattering amplitudes of the  $s$ -channel resonances within  $n=2$  shell for both  $\pi^- p \rightarrow K^0 \Lambda$  and  $\pi^- p \rightarrow \eta n$ , which have been listed in Table II. It should be pointed out that the contributions of  $s$ -channel resonances with a  $[70, 4^4 8]$  representation are forbidden in the  $\pi^- p \rightarrow K^0 \Lambda$  reaction due to the Moorhouse selection rule [73, 74]. Comparing these amplitudes of different resonances with each other, one can easily find which states are the main contributors to the reactions in the  $SU(6) \otimes O(3)$  symmetry limit.

Finally, the differential cross section  $d\sigma/d\Omega$  and polarization of final baryon  $P$  can be calculated by

$$\frac{d\sigma}{d\Omega} = \frac{(E_i + M_i)(E_f + M_f)}{64\pi^2 s(2M_i)(2M_f)} \frac{|\mathbf{q}|}{|\mathbf{k}|} \frac{1}{2} \times \sum_{\lambda_i, \lambda_f} |M_{\lambda_f, \lambda_i}|^2, \quad (12)$$

$$P = 2 \frac{\text{Im}[f(\theta)g^*(\theta)]}{|f(\theta)|^2 + |g(\theta)|^2},$$

where  $\lambda_i = \pm \frac{1}{2}$  and  $\lambda_f = \pm \frac{1}{2}$  are the helicities of the initial and final baryon states, respectively.

### III. CALCULATION AND ANALYSIS

#### A. Parameters

In the calculation, the universal value of harmonic oscillator parameter  $\alpha=0.4$  GeV is adopted. The masses of the  $u$ ,  $d$ , and  $s$  constituent quarks are adopted as  $m_u=m_d=330$  MeV and  $m_s=450$  MeV, respectively.

In our work, the  $s$ -channel resonance transition amplitude,  $O_R$ , is derived in the  $SU(6) \otimes O(3)$  symmetric quark model limit. In reality, the symmetry of  $SU(6) \otimes O(3)$  is generally broken due to, e.g., spin-dependent forces in the quark-quark interaction. As a result, configuration mixing would occur, which can produce an effect on our theoretical predictions.

TABLE III: Resonance masses  $M_R$  (MeV) and widths  $\Gamma_R$  (MeV) in this work compared with the world average value from the PDG [2].

resonance	$M_R$	$\Gamma_R$	$M_R$ (PDG)	$\Gamma_R$ (PDG)
$N(1535)S_{11}$	1524	124	$1535 \pm 10$	$150 \pm 25$
$N(1650)S_{11}$	1670	119	$1655^{+15}_{-10}$	$140 \pm 30$
$N(1520)D_{13}$	1515	125	$1515 \pm 5$	$115^{+10}_{-15}$
$N(1700)D_{13}$	1700	150	$1700 \pm 50$	$150^{+100}_{-50}$
$N(1675)D_{15}$	1685	140	$1675 \pm 5$	$150^{+15}_{-20}$
$N(1440)P_{11}$	1430	350	$1430 \pm 20$	$350 \pm 100$
$N(1710)P_{11}$	1710	200	$1710 \pm 30$	$100^{+150}_{-50}$
$N(1870)P_{11}$	1870	235	$1870 \pm 35$	$235 \pm 65$
$N(?)P_{13}$	2000	200	?	?
$N(1720)P_{13}$	1690	400	$1720^{+30}_{-20}$	$250^{+150}_{-100}$
$N(1900)P_{13}$	1900	250	$\sim 1900$	$\sim 250$
$N(?)P_{13}$	2040	200	?	?
$N(1680)F_{15}$	1680	130	$1685 \pm 5$	$130 \pm 10$
$N(1860)F_{15}$	1860	270	$1860^{+100}_{-40}$	$270^{+140}_{-50}$
$N(?)F_{15}$	2050	200	?	?
$N(?)F_{17}$	1990	200	?	?

TABLE IV: Extracted partial decay width ratios for  $N(1535)$  and  $N(1650)$  resonances compared with the values from the PDG [2].

Resonance	$\frac{\Gamma_{\eta N}}{\Gamma_{\pi N}}$ (ours)	$\frac{\Gamma_{\eta N}}{\Gamma_{\pi N}}$ (PDG)	$\frac{\Gamma_{K\Lambda}}{\Gamma_{\pi N}}$ (ours)	$\frac{\Gamma_{K\Lambda}}{\Gamma_{\pi N}}$ (PDG)
$N(1535)S_{11}$	1.57	$1.20^{+0.29}_{-0.62}$	/	/
$N(1650)S_{11}$	0.23	0.05-0.30	0.20	0.03-0.22

According to our previous studies of the  $\eta$  and  $\pi^0$  photoproduction on the nucleons [48, 49], we found the configuration mixings seem to be inevitable for the low-lying  $S$ -wave nucleon resonances  $N(1535)S_{11}$  and  $N(1650)S_{11}$ . Thus, in this work we also consider configuration mixing effects in the  $S$ -wave states and use the same mixing scheme as in our previous works [48, 49],

$$\begin{pmatrix} S_{11}(1535) \\ S_{11}(1650) \end{pmatrix} = \begin{pmatrix} \cos \theta_S & -\sin \theta_S \\ \sin \theta_S & \cos \theta_S \end{pmatrix} \begin{pmatrix} |70, 2^8, 1/2^-\rangle \\ |70, 4^8, 1/2^-\rangle \end{pmatrix}, \quad (13)$$

where  $\theta_S$  is the mixing angle. Then, the  $s$ -channel resonance transition amplitudes of the  $S$ -wave states  $N(1535)S_{11}$  and  $N(1650)S_{11}$  are related to the mixing angle  $\theta_S$ . These transition amplitudes have been worked out and listed in Tab. II. The mixing angle  $\theta_S$  has been determined by fitting the data. The determined value  $\theta_S \simeq 26.9^\circ$  is consistent with that suggested in our previous works [48, 49].

In the calculations, the quark-pseudoscalar-meson couplings are the overall parameters in the  $s$ - and  $u$ -channel transitions. However, they are not totally free ones. They can be related to the hadronic couplings via the Goldberger-Treiman relation [75]

$$g_{mNN} = \frac{g_A^m M_N}{F_m}, \quad (14)$$



TABLE V: Reduced  $\chi^2$  per data point of the full model and that with one resonance or one background switched off obtained in a global fit of the data of  $\pi^- p \rightarrow K^0 \Lambda$  and  $\pi^- p \rightarrow \eta n$ . The corresponding partial  $\chi^2$ s for the  $\pi^- p \rightarrow K^0 \Lambda$  (labeled with  $\chi_K^2$ ) and  $\pi^- p \rightarrow \eta n$  (labeled with  $\chi_\eta^2$ ) are also included.

	full model	$n$ -pole	$N(1535)S_{11}$	$N(1650)S_{11}$	$N(1520)D_{13}$	$N(1720)P_{13}$	$u$ -channel	$t$ -channel
$\chi^2$	5.98	14.96	265.03	24.88	14.53	5.99	15.79	15.03
$\chi_\eta^2$	8.54	13.36	466.86	40.31	24.52	8.07	18.09	10.49
$\chi_K^2$	2.78	16.95	12.75	5.58	2.05	3.39	12.92	20.70

where  $m$  stands for the pseudoscalar mesons,  $\eta$ ,  $\pi$  and  $K$ ;  $g_A^m$  is the axial vector coupling for the meson; and  $F_m$  is the meson decay constant, which can be related to  $f_m$  defined earlier by  $F_m = f_m / \sqrt{2}$ .

It should be pointed out that the  $\pi NN$  coupling constant  $g_{\pi NN}$  is a well-determined number,  $g_{\pi NN} = 13.48$ , thus, we fix it in our calculations. While for the other two coupling constants  $g_{K\Lambda}$  and  $g_{\eta NN}$ , there are larger uncertainties. We determine them by fitting the data of the  $\pi^- p \rightarrow K^0 \Lambda$ ,  $\eta n$  processes, respectively. We get that

$$g_{K\Lambda} \simeq 6.87, \quad g_{\eta NN} \simeq 2.50. \quad (15)$$

The coupling constant  $g_{\eta NN}$  extracted in present work is consistent with that extracted from the  $\eta$  meson photoproduction on nucleons in our previous work [48], and also in good agreement with the determinations in Refs. [58, 76–78]. And the coupling constant  $g_{K\Lambda}$  extracted by us is consistent with that extracted from the  $K$  meson photoproduction on nucleons in Refs. [37, 57, 79].

In the  $t$  channel of the  $\pi^- p \rightarrow K^0 \Lambda$  process, there are two free parameters,  $G_{Va}$  and  $g_{SP}g_{Sqq}$ , which come from  $K^*$  and  $\kappa$  exchanges, respectively. By fitting the data, we get  $G_{Va} \simeq 3.0$  and  $g_{SP}g_{Sqq} \simeq 36.4$ , which are close to our previous determinations in the  $K^- p$  scattering [71]. While, in the  $t$  channel of the  $\pi^- p \rightarrow \eta n$  process, the parameter from the  $a_0$  exchange  $g_{a_0\pi\eta}g_{a_0NN}$  are adopted a commonly used value  $g_{a_0\pi\eta}g_{a_0NN} \simeq 100$  based on Refs. [36, 80].

In the  $u$  channel, it is found that contributions from the  $n \geq 1$  shell resonances are negligibly small and insensitive to their masses. Thus, the  $n = 1$  and the  $n = 2$  shell resonances are treated as degeneration. In the calculations, we take  $M_1 = 1650$  MeV ( $M_2 = 1750$  MeV) for the degenerate mass of  $n = 1$  ( $n = 2$ ) shell resonances.

In the  $s$  channel, the masses and widths of the nucleon resonances are taken from the PDG [2], or the constituent quark model predictions [5] if no experimental data are available. For the main resonances, we allow their masses and widths to change in a proper range in order to better describe the data. The determined values are listed in Tab. III. It is found that the main resonance masses and widths extracted by us are in good agreement with the world average values from PDG [2]. One point should be emphasized that our global fits of the  $\pi^- p \rightarrow \eta n$ ,  $K^0 \Lambda$  reaction data seem to favour a broad width  $\Gamma \simeq 400$  MeV for  $N(1720)P_{13}$ , however, this width is much broader than  $\Gamma \simeq 120$  MeV extracted from the neutral pion photoproduction processes in our previous work [49]. A similar narrow width of  $N(1720)P_{13}$  was also found by the CLAS

Collaboration in the reaction  $ep \rightarrow ep'\pi^+\pi^-$  [81]. We will further discuss whether a narrow width state  $N(1720)P_{13}$  is allowed or not in the  $\pi^- p \rightarrow \eta n$ ,  $K^0 \Lambda$  reactions later.

Combining the extracted coupling constants,  $g_{K\Lambda}$  and  $g_{\eta NN}$ , and resonance masses, we further determine some partial width ratios of the main contributors  $N(1535)S_{11}$  and  $N(1650)S_{11}$  to the reactions, which have been listed in Tab. IV. From the table we can see that the partial width ratios  $\Gamma_{\eta N}/\Gamma_{\pi N}$  and  $\Gamma_{K\Lambda}/\Gamma_{\pi N}$  determined by us are close to the upper limit of the values from the PDG [2].

Finally, it should be pointed out that all adjustable parameters are determined by globally fitting the measured differential cross sections of the  $\pi^- p \rightarrow \eta n$ ,  $K^0 \Lambda$  processes. All the data sets used in our fits have been shown in Figs. 3 and 5. The reduced  $\chi^2$  per data point obtained in our fits has been listed in Tab. V. To clearly see the role of one component in the reactions, the  $\chi^2$ s with one resonance or one background switched off are also given in the table.

## B. $\pi^- p \rightarrow K^0 \Lambda$

The differential cross sections and total cross section of the  $\pi^- p \rightarrow K^0 \Lambda$  process compared with experimental data are shown in Figs. 1 and 2, respectively. From these figures, it is found that the experimental data in the c.m. energy range from threshold up to  $W \simeq 1.8$  GeV are reasonably described within the chiral quark model.

Obvious roles of the  $S$ -wave states  $N(1535)S_{11}$  and  $N(1650)S_{11}$  are seen in the reaction. The constructive interferences between  $N(1535)S_{11}$  and  $N(1650)S_{11}$  are crucial to reproduce the bump structure near threshold in the total cross section. Switching off the contributions of  $N(1535)S_{11}$  or  $N(1650)S_{11}$ , the cross sections around their mass thresholds are notably underestimated (see Figs. 2 and 3). It should be pointed out that in the symmetric quark model, the  $N(1650)S_{11}$  resonance corresponds to the  $[70, 4^8]$  representation. In the  $SU(6) \otimes O(3)$  symmetry limit, the contributions of  $N(1650)S_{11}$  should be forbidden in the  $\pi^- p \rightarrow K^0 \Lambda$  reaction due to the Moorhouse selection rule [73, 74]. The obvious evidence of  $N(1650)S_{11}$  in the  $\pi^- p \rightarrow K^0 \Lambda$  reaction further confirms that the  $SU(6) \otimes O(3)$  symmetry is broken, and the configuration mixing between  $N(1535)S_{11}$  and  $N(1650)S_{11}$  should be necessary as suggested in our previous studies of the meson photoproduction processes [48, 49].

Furthermore, some contributions from  $N(1720)P_{13}$  might be seen in the differential cross sections. At backward an-

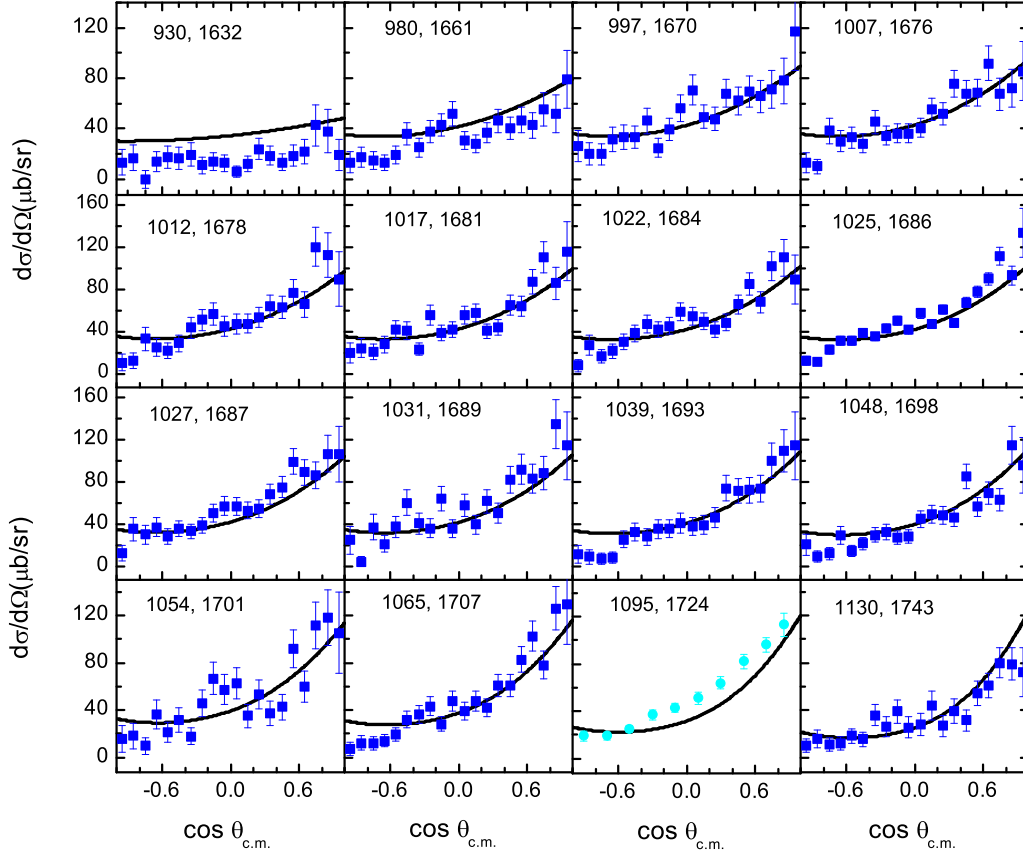


FIG. 1: Differential cross sections of the reaction  $\pi^- p \rightarrow K^0 \Lambda$  compared with the experimental data from Refs. [14] (solid squares) and [11] (solid circle). The first and second numbers in each figure correspond to the  $\pi^-$  beam momentum  $P_\pi$  (MeV) and the  $\pi N$  center-of-mass (c.m.) energy  $W$  (MeV), respectively.

gles, the differential cross sections are slightly underestimated without its contribution. For the large uncertainties of the data, here we can not obtain solid information on  $N(1720)P_{13}$ . If we adopt a narrow width  $\Gamma \approx 120$  MeV as suggested in our previous work [49], from Fig. 8 we see that the peak of the bump structure in the total cross section becomes sharper, and around the mass threshold of  $N(1720)P_{13}$  the differential cross sections at forward angles are enhanced significantly. Our theoretical predictions with a narrow width for  $N(1720)P_{13}$  are still consistent with the data within their uncertainties. Thus, to finally determine the properties of  $N(1720)P_{13}$ , we need more accurate measurements of the  $\pi^- p \rightarrow K^0 \Lambda$  reaction.

The  $n$ -pole,  $u$ - and  $t$ -channel backgrounds play crucial roles in the reaction as well. From the Figs. 2 and 3, one can see that switching off the  $u$ -channel contribution, the cross sections should be strongly overestimated; while switching off the  $t$ -channel contribution, the cross sections will be underestimated draftily. The  $n$ -pole has obvious effects on angle distributions of the cross sections in the whole energy region what we considered. Without the  $n$ -pole contribution, the dif-

ferential cross sections at forward angles should be notably underestimated, while those at backward angles should be notably overestimated.

In experiments, there are some old measurements for the  $\Lambda$  polarization of the  $\pi^- p \rightarrow K^0 \Lambda$  reaction [11]. In Fig. 4 we compare our chiral quark model predictions with the observations in the c.m. energy range  $W < 1.8$  GeV. We found that the experimental observations can be explained reasonably. It should be emphasized that our theoretical calculations seem to slightly underestimate the  $\Lambda$  polarization. This phenomenon also exist in the coupled-channel approach calculations [7]. Improved measurements and more reliable experimental data of the polarization are needed to clarify the discrepancies.

As a whole, obvious evidence of  $N(1535)S_{11}$  and  $N(1650)S_{11}$  are found in the  $\pi^- p \rightarrow K^0 \Lambda$  reaction, which is consistent with the recent analysis within an effective Lagrangian approach [45]. It should be emphasized that the  $N(1650)S_{11}$  resonance contributes to the reaction via the configuration mixing with  $N(1535)S_{11}$ . The determined mixing angle is  $\theta_5 \approx 26.9^\circ$ . Furthermore, remarkable contributions

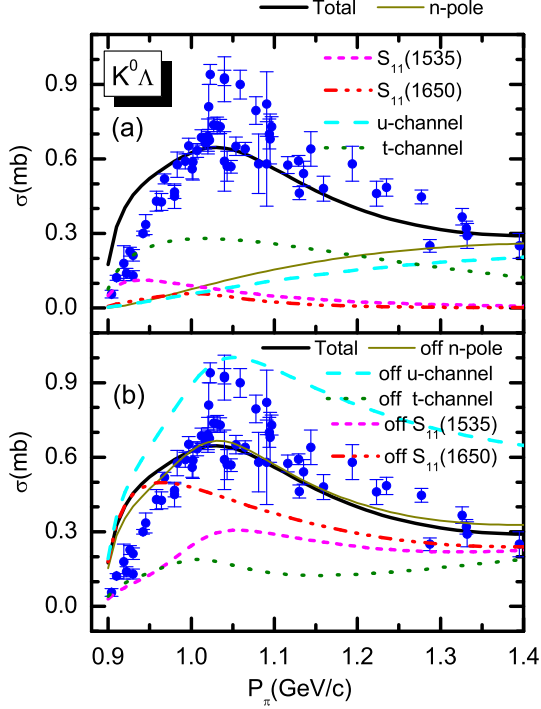


FIG. 2: Total cross section of the reaction  $\pi^- p \rightarrow K^0 \Lambda$  compared with experimental data from Ref. [15]. The bold solid curves correspond to the full model result. In figure (a), exclusive cross sections for  $S_{11}(1535)$ ,  $S_{11}(1650)$ , nucleon pole,  $u$  channel and  $t$  channel are indicated explicitly by the legends. In figure (b), the results by switching off the contributions of  $S_{11}(1535)$ ,  $S_{11}(1650)$ , nucleon pole,  $u$  channel and  $t$  channel are indicated explicitly by the legends.

from the backgrounds,  $n$ -pole,  $u$ - and  $t$ -channel, are found in the reaction. There might be sizeable contributions from  $N(1720)P_{13}$ , the present data can not determine whether it is a narrow or broad state. No clear evidence from the other nucleon resonances, such as  $N(1520)D_{13}$ ,  $N(1700)D_{13}$  and  $N(1710)P_{11}$ , is found in the reaction. Finally, it should be mentioned that the  $N(1710)P_{11}$  was considered as one of the main contributors to  $\pi^- p \rightarrow K^0 \Lambda$  in the literature [7, 25, 47], which is in disagreement with our prediction and that from Refs. [27, 28, 45].

### C. $\pi^- p \rightarrow \eta n$

The chiral quark model approach was first extended to the study of the reaction  $\pi^- p \rightarrow \eta n$  near threshold in our previous work [43]. For the unthoroughness of partial wave analysis for the  $n = 2$  shell resonances, and no considerations of the configuration mixing between  $N(1535)S_{11}$  and  $N(1650)S_{11}$ , we only obtained preliminary results. In this work, by combining the study of the reaction  $\pi^- p \rightarrow K^0 \Lambda$ , we present a comprehensive study of the  $\pi^- p \rightarrow \eta n$  process to better understand this reaction and extract more reliable properties of

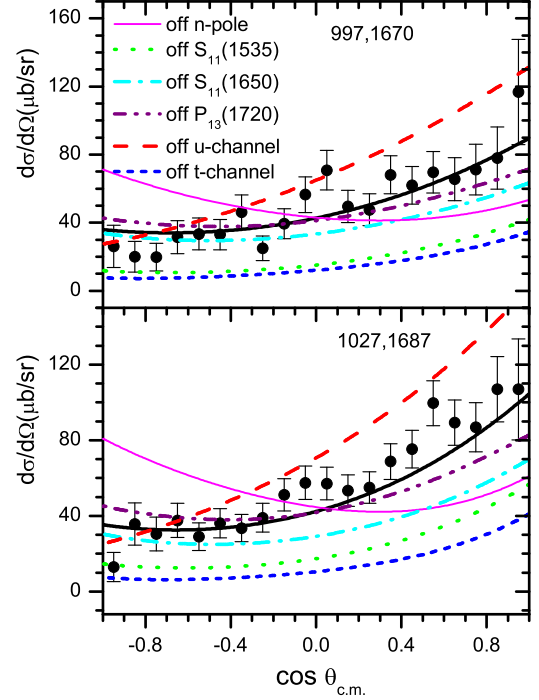


FIG. 3: Differential cross sections of the reaction  $\pi^- p \rightarrow K^0 \Lambda$  compared with experimental data [14] at two energy points  $P_\pi = 997, 1027$  MeV/c. The bold solid curves correspond to the full model result. The predictions by switching off the contributions from  $N(1535)S_{11}$ ,  $N(1650)S_{11}$ ,  $N(1720)P_{13}$ , and  $n$ -pole,  $u$ - and  $t$ -channel backgrounds are indicated explicitly by the legends in the figures.

nucleon resonances.

The differential cross sections and total cross section compared with the experimental data are shown in Figs. 5 and 6, respectively. From the figures, it is seen that the experimental data in the c.m. energy range from threshold up to  $W \simeq 1.8$  GeV can be reasonably described within the chiral quark model. Compared with our previous study in [43], the results in present work have an obvious improvement.

In the  $S$ -wave states, dominant role of  $N(1535)S_{11}$  can be found in the reaction. It is responsible for the first hump around  $P_\pi \simeq 0.76$  GeV/c ( $W \simeq 1.5$  GeV). Without the  $N(1535)S_{11}$  contribution, the first hump disappears completely. In addition, a sizeable contribution from  $N(1650)S_{11}$  can be seen from Figs. 6 and 7. Around the first hump,  $N(1650)S_{11}$  has obvious destructive interferences with  $N(1535)S_{11}$ , which is consistent with our previous study [43]. In the total cross section there seems to exist another small bump structure around  $P_\pi \simeq 1.0$  GeV/c ( $W \simeq 1.7$  GeV). Based on our calculations shown in Fig. 6, the interferences between  $N(1650)S_{11}$ ,  $N(1535)S_{11}$  and  $u$ -channel background might be responsible for the this structure, which is different from our previous prediction [43]. Our results in present work are consistent with the those analyses within the coupled-channel approaches [27, 32, 40, 41].

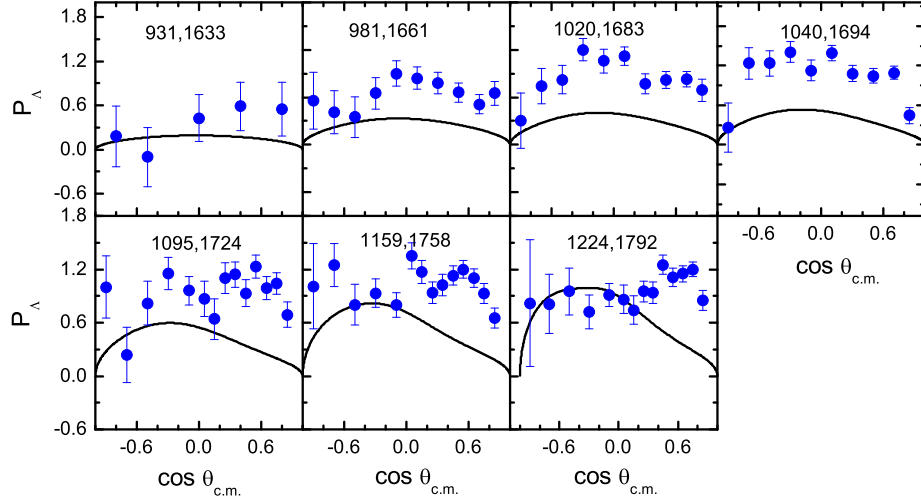


FIG. 4:  $\Lambda$  polarization of the  $\pi^- p \rightarrow K^0 \Lambda$  reaction compared with experimental data [11].

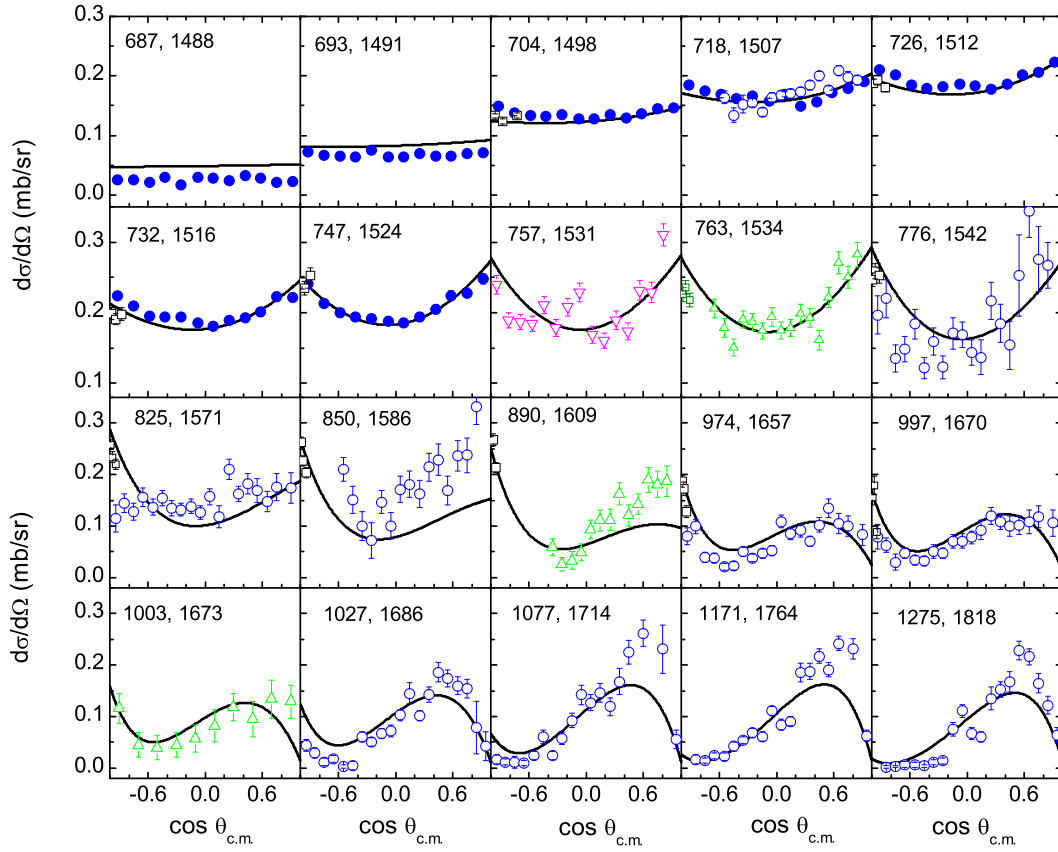


FIG. 5: Differential cross sections of the reaction  $\pi^- p \rightarrow \eta n$  compared with the experimental data from Refs. [17] (open circle), [18] (open up-triangles), [19] (open down-triangles), [20] (open squares) and the recent experiment presented in Ref. [16] (solid circles). The first and second numbers in each figure correspond to the  $\pi^-$  beam momentum  $P_\pi$  (MeV) and the  $\pi N$  center-of-mass (c.m.) energy  $W$  (MeV), respectively.



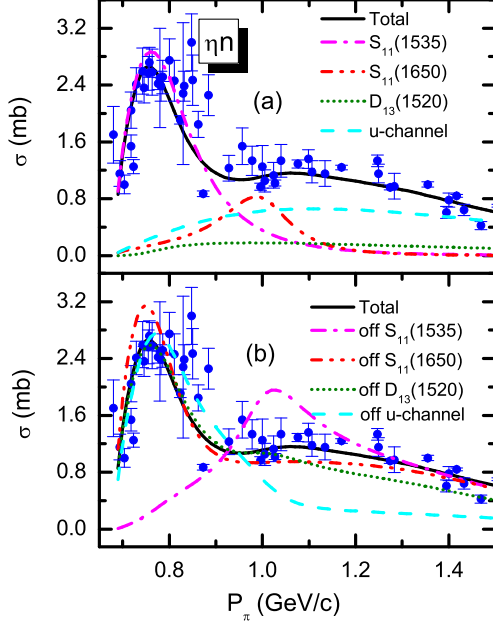


FIG. 6: Total cross section of the reaction  $\pi^- p \rightarrow \eta n$  compared with experimental data [15]. The bold solid curves correspond to the full model result. In figure (a), exclusive cross sections for  $S_{11}(1535)$ ,  $S_{11}(1650)$ ,  $N(1520)D_{13}$ , and  $u$  channel are indicated explicitly by the legends. In figure (b), the results by switching off the contributions of  $S_{11}(1535)$ ,  $S_{11}(1650)$ ,  $N(1520)D_{13}$ , and  $u$  channel are indicated explicitly by the legends.

In the  $D$ -wave states,  $N(1520)D_{13}$  plays an important role in the reaction, which can be obviously seen in the differential cross sections. Its interferences with the  $N(1535)S_{11}$  and backgrounds is crucial to produce the correct shape of the differential cross sections in the whole energy region what we have considered. From the Fig. 5 one can see that without the  $N(1520)D_{13}$  contribution, the shape of the differential cross sections changes significantly. However, no obvious effects of  $N(1520)D_{13}$  on the total cross section can be found in the  $\pi^- p \rightarrow \eta n$  reaction. This feature was mentioned in Refs. [35, 36]. It should be pointed out that to well describe the data, a large amplitude of  $N(1520)D_{13}$  in the reaction is needed, which is about a factor of 2.18 larger than that derived in the  $SU(6) \otimes O(3)$  limit, which can not be explained with configuration mixing effects.

With the energy increasing, the  $u$ -channel background become more and more important in the reaction. Its large effects on both total cross section and differential cross sections can be notably seen in the energy region  $P_\pi > 0.8$  GeV/c ( $W > 1.5$  GeV). Its interferences with the resonances  $N(1650)S_{11}$  and  $N(1535)S_{11}$  are responsible for the second bump structure around  $P_\pi \approx 1.0$  GeV/c ( $W \approx 1.7$  GeV).

No determined evidence of the other resonances, such as  $D(1700)D_{13}$ ,  $D(1675)D_{13}$ , and higher  $P$ -,  $F$ -wave resonances

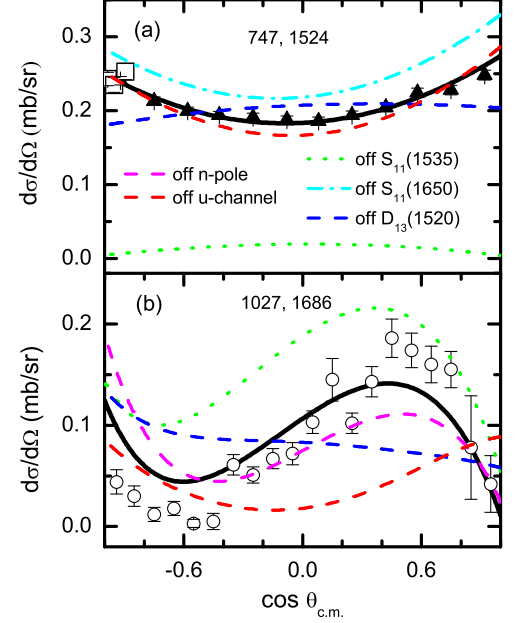


FIG. 7: Differential cross sections of the reaction  $\pi^- p \rightarrow \eta n$  compared with experimental data at two energy points  $P_\pi = 747, 1027$  MeV/c. The bold solid curves correspond to the full model result. The predictions by switching off the contributions from  $N(1535)S_{11}$ ,  $N(1650)S_{11}$ ,  $N(1520)D_{13}$ , and  $n$ -pole,  $u$ -channel backgrounds are indicated explicitly by the legend in the figures.

is found in the reaction. The background contributions from  $n$ -pole and  $t$ -channel are less important to the reaction.

We should point out that some analyses of this reaction suggest the need of the  $N(1710)P_{11}$  resonance [7, 27, 29, 33]. However, according to our analysis, no obvious  $N(1710)P_{11}$  contribution is required for a good description of the experimental observations. Meanwhile, our analysis indicates that  $N(1720)P_{13}$  might have some effects on the cross sections. According to our results from partial wave analysis (see Tab. II), in the  $SU(6) \otimes O(3)$  symmetry limit the scattering amplitudes of  $N(1720)P_{13}$  are much larger than those of  $N(1710)P_{11}$  around  $W = 1.7$  GeV. Thus, the role of  $N(1720)P_{13}$  might be more obvious than that of  $N(1710)P_{11}$  if they are indeed seen in the reaction, which is consistent with the chiral quark model study in Ref. [44]. In this work, we find that the role of  $N(1720)P_{13}$  is sensitive to its width. If we adopt a broad width of  $\Gamma \approx 400$  MeV obtained by fitting the data, the contributions of  $N(1720)P_{13}$  to the reaction are negligibly small. However, if we adopt a narrower width  $\Gamma \approx 120$  MeV as suggested in our previous work by a study of the  $\pi^0$  photo-production [49], we find that the second bump structure in the total cross section become more obvious, while around  $W = 1.7$  GeV the cross sections at backward angles are enhanced significantly. It should be emphasized that although our theoretical results seem to become bad compared with the data with

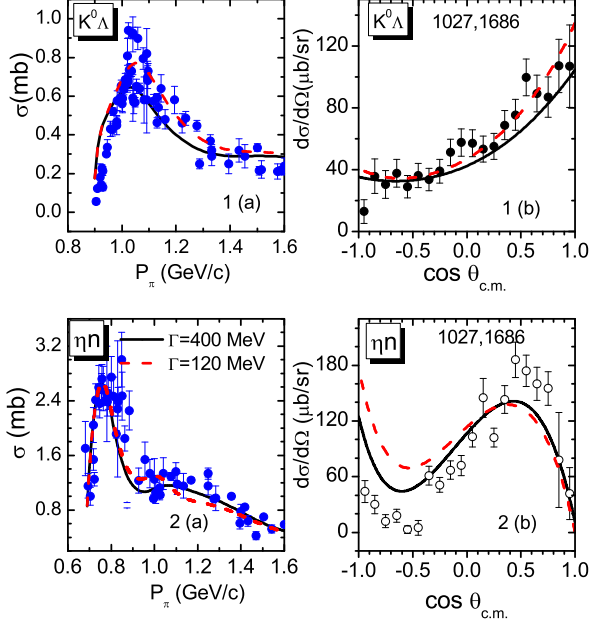


FIG. 8: Predictions for the  $\pi^- p \rightarrow K^0 \Lambda$  and  $\eta n$  reactions with a narrow width  $\Gamma = 120$  MeV and a broad width  $\Gamma = 400$  MeV for the resonance  $N(1720)P_{13}$ , respectively. The total cross sections for  $\pi^- p \rightarrow K^0 \Lambda$  and  $\eta n$  are plotted in 1(a) and 2(a), respectively. While the differential cross sections at  $P_\pi=1027$  MeV/c for  $\pi^- p \rightarrow K^0 \Lambda$  and  $\eta n$  are plotted in 1(b) and 2(b), respectively. The solid curves stand for the results with a broad width  $\Gamma = 400$  MeV, while the dashed curves for the results with a narrow width  $\Gamma = 120$  MeV.

a narrow width of  $N(1720)P_{13}$ , we can not exclude this possibility because the old data obtained many years ago might be problematic for its uncontrollable uncertainties [23]. New observations of the  $\pi^- p \rightarrow \eta n$  reaction are urgently needed to better understand the properties of nucleon resonances.

In brief,  $N(1535)S_{11}$  play a dominant role in the  $\pi^- p \rightarrow \eta n$  reaction near  $\eta$  production threshold. In this low energy region,  $N(1650)S_{11}$  has notable destructive interferences with  $N(1535)S_{11}$ . The  $u$ -channel background also plays a crucial role in the reaction. The interferences between  $N(1650)S_{11}$  and  $u$ -channel background might be responsible for the second bump structure around  $P_\pi \simeq 1.0$  GeV/c ( $W \simeq 1.7$  GeV).  $N(1520)D_{13}$  is crucial to describe the differential cross sections, although it has small contributions to the total cross section. To confirm the role of  $N(1720)P_{13}$  in the reaction, new accurate measurements are urgently needed in the c.m. energy range  $W \simeq 1.5 - 1.8$  GeV. No obvious evidences of  $N(1700)D_{13}$ ,  $N(1675)D_{15}$ ,  $N(1710)P_{11}$ , and  $N(1680)F_{15}$  are found in the  $\pi^- p \rightarrow \eta n$  reaction, which is in disagreement with the predictions in [7, 27, 29, 33], where the authors predicted the  $N(1710)P_{11}$  resonance is needed to explain the reaction.

#### IV. SUMMARY

In this work, a combined study of the  $\pi^- p \rightarrow K^0 \Lambda$  and  $\eta n$  have been carried out within a chiral quark model. We have

achieved reasonable descriptions of the data in the c.m. energy range from threshold up to  $W \simeq 1.8$  GeV.

Obvious evidence of the  $S$ -wave nucleon resonances  $N(1535)S_{11}$  and  $N(1650)S_{11}$  is found in both of these two reactions.  $N(1650)S_{11}$  contributes to the  $\pi^- p \rightarrow K^0 \Lambda$  reaction through configuration mixing with  $N(1535)S_{11}$ . The determined mixing angle is  $\theta_s \simeq 26.9^\circ$ , which is consistent with that extracted from  $\eta$  and  $\pi^0$  photoproduction processes in our previous works [48, 49]. Furthermore, the partial width ratios  $\Gamma_{\eta N}/\Gamma_{\pi N}$  and  $\Gamma_{K\Lambda}/\Gamma_{\pi N}$  for these  $S$ -wave states are extracted from the reactions, which are close to the upper limit of the average values from the PDG [2]. Obvious role of the  $D$ -wave state  $N(1520)D_{13}$  is found in  $\pi^- p \rightarrow \eta n$  reaction, which has large effects on the differential cross sections although its effects on the total cross section are tiny. It should be pointed out that the effects of  $N(1520)D_{13}$  on the  $\pi^- p \rightarrow K^0 \Lambda$  are negligibly small.

The backgrounds play remarkable roles in these two strong interaction processes. In the  $\pi^- p \rightarrow K^0 \Lambda$  process, the  $u$ -,  $t$ -channel, and  $n$ -pole backgrounds have notable contributions to the cross sections. While in the  $\pi^- p \rightarrow \eta n$  process, the  $u$ -channel background plays a crucial role in the higher energy region  $W > 1.5$  GeV.

The role of  $P$ -wave state  $N(1720)P_{13}$  should be further confirmed by future experiments. In present work, the data seem to favour a broad width  $\Gamma \simeq 400$  MeV for  $N(1720)P_{13}$ . However, our previous study of the  $\pi^0$  photoproduction process indicates that the  $N(1720)P_{13}$  might have a narrow width of  $\Gamma \simeq 120$  MeV [49]. If  $N(1720)P_{13}$  has a broad width of  $\Gamma \simeq 400$  MeV, its contributions to the reactions  $\pi^- p \rightarrow K^0 \Lambda$  and  $\eta n$  should be negligibly small. However, if  $N(1720)P_{13}$  has a narrow width of  $\Gamma \simeq 120$  MeV, its contributions to the reactions are obvious, which can be seen from both the total cross section and differential cross sections. The present data of the  $\pi^- p \rightarrow K^0 \Lambda$  allow the appearance of a narrow  $N(1720)P_{13}$  resonance within the uncertainties. However, when using a narrow width of  $N(1720)P_{13}$  in the  $\pi^- p \rightarrow \eta n$  reaction, our theoretical results are notably larger than the data at the backward angles. Improved measurements and more reliable experimental data of the  $\pi^- p \rightarrow K^0 \Lambda$  and  $\eta n$  reactions are needed to clarify the puzzle about  $N(1720)P_{13}$ .

Finally it should be pointed out that no obvious evidences of  $N(1700)D_{13}$ ,  $N(1675)D_{15}$ ,  $N(1710)P_{11}$ , and  $N(1680)F_{15}$  are found in the  $\pi^- p \rightarrow K^0 \Lambda$  and  $\eta n$  reactions, although they sit on the energy range what we considered.

#### Acknowledgments

This work is partly supported by the National Natural Science Foundation of China (Grants No. 11075051 and No. 11375061), the Hunan Provincial Natural Science Foundation (Grant No. 13JJ1018), and the Hunan Provincial Innovation Foundation for Postgraduate.

- 
- [1] E. Klempt and J. M. Richard, Baryon spectroscopy, *Rev. Mod. Phys.* **82**, 1095 (2010).
- [2] K. A. Olive *et al.* [Particle Data Group Collaboration], Review of Particle Physics, *Chin. Phys. C* **38**, 090001 (2014).
- [3] N. Isgur and G. Karl, P Wave Baryons in the Quark Model, *Phys. Rev. D* **18**, 4187 (1978).
- [4] N. Isgur and G. Karl, Hyperfine Interactions in Negative Parity Baryons, *Phys. Lett. B* **72**, 109 (1977); *Phys. Rev. D* **19**, 2653 (1979); **23**, 817 (1981); **20**, 1191 (1979).
- [5] S. Capstick and N. Isgur, Baryons in a Relativized Quark Model with Chromodynamics, *Phys. Rev. D* **34**, 2809 (1986).
- [6] W. J. Briscoe, M. Döring, H. Haberzettl, D. M. Manley, M. Naruki, I. I. Strakovsky and E. S. Swanson, Physics opportunities with meson beams, *Eur. Phys. J. A* **51**, 129 (2015).
- [7] D. Ronchen *et al.*, Coupled-channel dynamics in the reactions  $\pi N \rightarrow \pi N, \eta N, K\Lambda, K\Sigma$ , *Eur. Phys. J. A* **49**, 44 (2013).
- [8] L. Bertanza, P. L. Connolly, B. B. Culwick, F. R. Eisler, T. Morris, R. B. Palmer, A. Prodel and N. P. Samios,  $\Lambda K^0$  production by pions on protons, *Phys. Rev. Lett.* **8**, 332 (1962).
- [9] J. J. Jones *et al.*, Total cross-sections for  $\pi^- p \rightarrow \Lambda K^0$  from threshold to 1.13 gev/c, *Phys. Rev. Lett.* **26**, 860 (1971).
- [10] T. M. Knasel *et al.*, Experimental study of the reaction  $\pi^- p \rightarrow \Lambda K^0$  at beam momenta between 930 and 1130 MeV/c, *Phys. Rev. D* **11**, 1 (1975).
- [11] R. D. Baker *et al.*, The Reaction  $\pi^- p \rightarrow K^0 \Lambda^0$  Up to 1334 MeV/c, *Nucl. Phys. B* **141**, 29 (1978).
- [12] D. H. Saxon *et al.*, The Reaction  $\pi^- p \rightarrow K^0 \Lambda^0$  Up to 2375 MeV/c: New Results and Analysis, *Nucl. Phys. B* **162**, 522 (1980).
- [13] T. O. Binford, M. L. Good, V. G. Lind, D. Stern, R. Krauss and E. Dettman, Production of lambda-neutral and sigma-neutral hyperons by pions of beam momenta 1.12-1.32 bev/c, *Phys. Rev.* **183**, 1134 (1969).
- [14] B. Nelson *et al.*, Search for structure in  $\pi^- p \rightarrow K^0 \Lambda^0$  at sigma k threshold, *Phys. Rev. Lett.* **31**, 901 (1973).
- [15] A. Baldini, V. Flaminio, W. G. Moorhead, D. R. O. Morrison and H. Schopper, Numerical Data And Functional Relationships In Science And Technology. Grp. 1: Nuclear And Particle Physics. Vol. 12: Total Cross-sections For Reactions Of High-energy Particles (including Elastic, Topological, Inclusive And Exclusive Reactions). Subvol, BERLIN, GERMANY: SPRINGER (1988) 419 P. (LANDOLT-BOERNSTEIN. NEW SERIES, 1/12A)
- [16] S. Prakhov *et al.*, Measurement of  $\pi^- p \rightarrow \eta n$  from threshold to  $P_{\pi^-} = 747$  MeV/c, *Phys. Rev. C* **72**, 015203 (2005).
- [17] R. M. Brown *et al.*, Differential Cross-sections For The Reaction  $\pi^- p \rightarrow \eta n$  Between 724 MeV/c And 2723 MeV/c, *Nucl. Phys. B* **153**, 89 (1979).
- [18] W. Deinet, H. Mueller, D. Schmitt, H. M. Staudenmaier, S. Buniatov and E. Zavattini, Differential and total cross-sections for  $\pi^- p \rightarrow \eta n$  from 718 to 1050 MeV/c, *Nucl. Phys. B* **11**, 495 (1969).
- [19] J. Feltesse, R. Ayed, P. Bareyre, P. Borgeaud, M. David, J. Ernewein, Y. Lemoigne and G. Villet, The Reaction  $\pi^- p \rightarrow \eta n$  Up to  $P_{\pi^-} = 450$  MeV/c: Experimental Results and Partial Wave Analysis, *Nucl. Phys. B* **93**, 242 (1975).
- [20] N. C. Debenham *et al.*, Backward  $\pi^- p$  Reactions Between 0.6 GeV/c and 1 GeV/c, *Phys. Rev. D* **12**, 2545 (1975).
- [21] F. Bulos *et al.*, Charge exchange and production of eta mesons and multiple neutral pions in  $\pi^- p$  reactions between 654 and 1247 MeV/c, *Phys. Rev.* **187**, 1827 (1969).
- [22] W. B. Richards *et al.*, Production and neutral decay of the eta meson in  $\pi^- p$  collisions, *Phys. Rev. D* **1**, 10 (1970).
- [23] M. Clajus and B. M. K. Nefkens, The  $\pi^- p \rightarrow \eta n$  database, *PiN Newsl.* **7**, 76 (1992).
- [24] T. Hyodo, S. i. Nam, D. Jido and A. Hosaka, Detailed analysis of the chiral unitary model for meson baryon scatterings with flavor SU(3) breaking effects, *Prog. Theor. Phys.* **112**, 73 (2004).
- [25] M. Shrestha and D. M. M. Manley, Partial-Wave Analysis of  $\pi^- p \rightarrow \eta n$  and  $\pi^- p \rightarrow K^0 \Lambda$  Reactions, *Phys. Rev. C* **86**, 045204 (2012).
- [26] M. Shrestha and D. M. Manley, Multichannel parametrization of  $\pi N$  scattering amplitudes and extraction of resonance parameters, *Phys. Rev. C* **86**, 055203 (2012).
- [27] G. Penner and U. Mosel, Vector meson production and nucleon resonance analysis in a coupled channel approach for energies  $m_N < \sqrt{s} < 2$  GeV. I: Pion induced results and hadronic parameters, *Phys. Rev. C* **66**, 055211 (2002).
- [28] V. Shklyar, H. Lenske and U. Mosel, A Coupled-channel analysis of  $K\Lambda$  production in the nucleon resonance region, *Phys. Rev. C* **72**, 015210 (2005).
- [29] V. Shklyar, H. Lenske and U. Mosel,  $\eta$ -meson production in the resonance-energy region, *Phys. Rev. C* **87**, 015201 (2013).
- [30] M. Sotona and J. Zofka, Elementary Amplitudes of the Process  $\pi^- p \rightarrow K^0 \Lambda$ , *Prog. Theor. Phys.* **81**, 160 (1989).
- [31] T. Feuster and U. Mosel, A Unitary model for meson nucleon scattering, *Phys. Rev. C* **58**, 457 (1998).
- [32] V. Shklyar, G. Penner and U. Mosel, Spin 5/2 resonance contributions to the pion induced reactions for energies  $\sqrt{s} \leq 2.0$  GeV, *Eur. Phys. J. A* **21**, 445 (2004).
- [33] V. Shklyar, H. Lenske and U. Mosel, eta-photoproduction in the resonance energy region, *Phys. Lett. B* **650**, 172 (2007).
- [34] R. A. Arndt, W. J. Briscoe, I. I. Strakovsky, R. L. Workman and M. M. Pavan, Dispersion relation constrained partial wave analysis of  $\pi N$  elastic and  $\pi N \rightarrow \eta N$  scattering data: The Baryon spectrum, *Phys. Rev. C* **69**, 035213 (2004).
- [35] R. A. Arndt, W. J. Briscoe, T. W. Morrison, I. I. Strakovsky, R. L. Workman and A. B. Gridnev, Low-energy eta N interactions: Scattering lengths and resonance parameters, *Phys. Rev. C* **72**, 045202 (2005).
- [36] A. M. Gasparyan, J. Haidenbauer, C. Hanhart and J. Speth, Pion nucleon scattering in a meson exchange model, *Phys. Rev. C* **68**, 045207 (2003).
- [37] B. Julia-Diaz, B. Saghai, T.-S. H. Lee and F. Tabakin, Dynamical coupled-channel approach to hadronic and electromagnetic production of kaon-hyperon on the proton, *Phys. Rev. C* **73**, 055204 (2006).
- [38] W. T. Chiang, B. Saghai, F. Tabakin and T. S. H. Lee, Dynamical coupled-channel model of kaon-hyperon interactions, *Phys. Rev. C* **69**, 065208 (2004).
- [39] T. P. Vrana, S. A. Dytman and T. S. H. Lee, Baryon resonance extraction from pi N data using a unitary multichannel model, *Phys. Rept.* **328**, 181 (2000).
- [40] J. Durand, B. Julia-Diaz, T.-S. H. Lee, B. Saghai and T. Sato, Insights into the  $\pi^- p \rightarrow \eta n$  reaction mechanism, *Int. J. Mod. Phys. A* **24**, 553 (2009).
- [41] J. Durand, B. Julia-Diaz, T.-S. H. Lee, B. Saghai and T. Sato, Coupled-channels study of the  $\pi^- p \rightarrow \eta n$  process, *Phys. Rev. C* **78**, 025204 (2008).
- [42] A. V. Anisovich, R. Beck, E. Klempt, V. A. Nikonov, A. V. Sarantsev, U. Thoma and Y. Wunderlich, Study of ambiguities in  $\pi^- p \rightarrow \Lambda K^0$  scattering amplitudes, *Eur. Phys. J. A*

- 49, 121 (2013).
- [43] X. H. Zhong, Q. Zhao, J. He and B. Saghai, Study of  $\pi^- p \rightarrow \eta n$  at low energies in a chiral constituent quark model," Phys. Rev. C **76**, 065205 (2007).
- [44] J. He and B. Saghai, Combined study of  $\gamma p \rightarrow \eta p$  and  $\pi^- p \rightarrow \eta n$  in a chiral constituent quark approach, Phys. Rev. C **80**, 015207 (2009).
- [45] C. Z. Wu, Q. F. Lü, J. J. Xie and X. R. Chen, Nucleon resonances in the  $\pi^- p \rightarrow K^0 \Lambda$  reaction near threshold, Commun. Theor. Phys. **63**, 215 (2015).
- [46] Q. F. Lü, X. H. Liu, J. J. Xie and D. M. Li, The near threshold  $\pi^- p \rightarrow \eta n$  reaction in an effective Lagrangian approach, Mod. Phys. Lett. A **29**, 1450012 (2014).
- [47] S. Ceci, A. Svarc and B. Zauner, The Re-analysis of the 1700-MeV structure of the  $P_{11}$  partial wave using the  $\pi N \rightarrow K \Lambda$  production data, Few Body Syst. **39**, 27 (2006).
- [48] X. H. Zhong and Q. Zhao,  $\eta$  photoproduction on the quasi-free nucleons in the chiral quark model, Phys. Rev. C **84**, 045207 (2011).
- [49] L. Y. Xiao, X. Cao and X. H. Zhong, Neutral pion photoproduction on the nucleon in a chiral quark model, Phys. Rev. C **92**, 035202 (2015).
- [50] B. C. Liu and B. S. Zou, Mass and K Lambda coupling of  $N^*(1535)$ , Phys. Rev. Lett. **96**, 042002 (2006).
- [51] B. S. Zou, Strangeness in the proton and  $N^*(1535)$ , Nucl. Phys. A **790**, 110 (2007).
- [52] L. S. Geng, E. Oset, B. S. Zou and M. Doring, The Role of the  $N^*(1535)$  in the  $J/\psi \rightarrow \bar{p} \eta p$  and  $J/\psi \rightarrow \bar{p} K^+ \Lambda$  reactions, Phys. Rev. C **79**, 025203 (2009).
- [53] T. Inoue, E. Oset and M. J. Vicente Vacas, Chiral unitary approach to  $S$  wave meson baryon scattering in the strangeness  $S = 0$  sector, Phys. Rev. C **65**, 035204 (2002).
- [54] J. Nieves and E. Ruiz Arriola, The  $S_{11}$ - $N(1535)$  and  $-N(1650)$  resonances in meson baryon unitarized coupled channel chiral perturbation theory, Phys. Rev. D **64**, 116008 (2001).
- [55] M. Doring and K. Nakayama, The Phase and pole structure of the  $N^*(1535)$  in  $\pi N \rightarrow \pi N$  and  $\gamma N \rightarrow \pi N$ , Eur. Phys. J. A **43**, 83 (2010).
- [56] Z. P. Li, The Threshold pion photoproduction of nucleons in the chiral quark model, Phys. Rev. D **50**, 5639 (1994).
- [57] Z. P. Li, The Kaon photoproduction of nucleons in the chiral quark model, Phys. Rev. C **52**, 1648 (1995).
- [58] Z. P. Li, The Eta photoproduction of nucleons and the structure of the resonance  $S_{11}(1535)$  in the quark model, Phys. Rev. D **52**, 4961 (1995) doi:10.1103/PhysRevD.52.4961 [nucl-th/9506033].
- [59] Z. P. Li, H. X. Ye and M. H. Lu, A Unified approach to pseudoscalar meson photoproductions off nucleons in the quark model, Phys. Rev. C **56**, 1099 (1997).
- [60] Q. Zhao, J. S. Al-Khalili, Z. P. Li and R. L. Workman, Pion photoproduction on the nucleon in the quark model, Phys. Rev. C **65**, 065204 (2002).
- [61] Q. Zhao, Z. P. Li and C. Bennhold, Vector meson photoproduction with an effective Lagrangian in the quark model, Phys. Rev. C **58**, 2393 (1998).
- [62] Q. Zhao, J. S. Al-Khalili and C. Bennhold, Quark model predictions for  $K^*$  photoproduction on the proton, Phys. Rev. C **64**, 052201 (2001).
- [63] Q. Zhao, Z. P. Li and C. Bennhold,  $\Omega$  and  $\rho$  photoproduction with an effective quark model Lagrangian, Phys. Lett. B **436**, 42 (1998).
- [64] Z. P. Li and B. Saghai, Study of the baryon resonances structure via eta photoproduction, Nucl. Phys. A **644**, 345 (1998).
- [65] B. Saghai and Z. P. Li, Quark model study of the eta photoproduction: Evidence for a new  $S_{11}$  resonance?, Eur. Phys. J. A **11**, 217 (2001).
- [66] Q. Zhao, B. Saghai and Z. P. Li, Quark model approach to the eta meson electroproduction on the proton, J. Phys. G **28**, 1293 (2002) [nucl-th/0011069].
- [67] J. He, B. Saghai and Z. P. Li, Study of  $\eta$  photoproduction on the proton in a chiral constituent quark approach via one-gluon-exchange model, Phys. Rev. C **78**, 035204 (2008).
- [68] X. H. Zhong and Q. Zhao,  $\eta'$  photoproduction on the nucleons in the quark model, Phys. Rev. C **84**, 065204 (2011).
- [69] L. Y. Xiao and X. H. Zhong, Low-energy  $K^- p \rightarrow \Lambda \eta$  reaction and the negative parity  $\Lambda$  resonances, Phys. Rev. C **88**, 065201 (2013).
- [70] X. H. Zhong and Q. Zhao, The  $K^- p \rightarrow \Sigma^0 \pi^0$  reaction at low energies in a chiral quark model, Phys. Rev. C **79**, 045202 (2009).
- [71] X. H. Zhong and Q. Zhao, Low energy reactions  $K^- p \rightarrow \Sigma^0 \pi^0$ ,  $\Lambda \pi^0$ ,  $\bar{K}^0 n$  and the strangeness  $S = -1$  hyperons, Phys. Rev. C **88**, 015208 (2013).
- [72] J. Hamilton and W. S. Woolcock, Determination of Pion-Nucleon Parameters and Phase Shifts by Dispersion Relations, Rev. Mod. Phys. **35**, 737 (1963).
- [73] R. G. Moorhouse, Photoproduction Of  $N^*$  resonances in the quark model, Phys. Rev. Lett. **16**, 772 (1966).
- [74] Q. Zhao and F. E. Close, Quarks, diquarks and QCD mixing in the  $N^*$  resonance spectrum, Phys. Rev. D **74**, 094014 (2006).
- [75] M. L. Goldberger and S. B. Treiman, Decay of the pi meson, Phys. Rev. **110**, 1178 (1958).
- [76] J. Piekarewicz, Off-shell behavior of the  $\pi$ - $\eta$  mixing amplitude, Phys. Rev. C **48**, 1555 (1993).
- [77] L. Tiator, C. Bennhold and S. S. Kamalov, The Eta N N coupling in eta photoproduction, Nucl. Phys. A **580**, 455 (1994).
- [78] S. L. Zhu, The  $\eta NN$  coupling constant, Phys. Rev. C **61**, 065205 (2000).
- [79] W. T. Chiang, F. Tabakin, T. S. H. Lee and B. Saghai, Coupled channel study of  $\gamma p \rightarrow K^+ \Lambda$ , Phys. Lett. B **517**, 101 (2001).
- [80] O. Krehl, C. Hanhart, S. Krewald and J. Speth, What is the structure of the Roper resonance?, Phys. Rev. C **62**, 025207 (2000).
- [81] M. Ripani *et al.* [CLAS Collaboration], Measurement of  $ep \rightarrow e' p \pi^+ \pi^-$  and baryon resonance analysis, Phys. Rev. Lett. **91**, 022002 (2003).